Small Clusters of Water Adsorbed on the Bilayer-Terminated Ice Surface: Infrared Reflection Adsorption Spectra and Quantum Chemical Calculations

Alexander Pelmenschikov*,† and Hirohito Ogasawara‡

Department of Physics, Stockholm University, SCFAB, SE-106 91 Stockholm, Sweden, and The Institute of Physical and Chemical Research (RIKEN), 2-1 Hirosawa, Wako, Saitama 351-01, Japan

Received: August 1, 2001; In Final Form: January 3, 2002

Combining infrared reflection adsorption spectroscopy and ab initio quantum chemical methods we study adsorption of water on the "bilayer terminated" surface of ice film grown on a Ru(001) substrate. The adsorption was performed at 38 K with gradual increase of the coverage from 0.14 to 0.42 ML. Only three observed infrared bands, which are associated with the free OH groups, could be used for analysis of the structure: the OH stretching bands at 3720, 3695, and 3665 cm^{-1}. The calculated frequencies permit the assignment of these bands to the OH stretching vibrations of the single water molecules stabilized at the terminal OH groups (3720 cm^{-1}), the terminal OH groups of the bilayer surface (3695 cm^{-1}), and the terminal OH groups acting as a proton acceptor toward adsorbed water species (3665 cm^{-1}). Our calculations show that at the submonolayer coverage of water the lateral H-bonding interaction between the adsorbed molecules should lead to the aggregation of these molecules into small clusters. The structure of these clusters is significantly different from that of the ice, which results in the formation of disordered adsorption layer. This result suggests that upon adsorption of water the growth of the ice should occur by successive phase transition from the disordered adsorption layer to the bilayer.

Introduction

At very low temperature and ultrahigh vacuum, progressive adsorption of water on close-packed metal surfaces leads to the formation of a two-dimensional (2D) lattice of H-bonded water molecules known as a "bilayer ice".[1] The studies of the structure and growth of this 2D lattice are of important significance[1−6] for understanding the elementary mechanisms of water−metal and water−water interactions. At very low coverage the adsorption is mainly governed by the water−metal interaction; although for Pt(111) it may be complicated by water clustering due to a very low diffusion barrier for isolated water molecules.[3,7] At a higher coverage, when the water molecules form the bilayer ice with a large domain size, the adsorption is dominated by the H-bonding interaction with the ice surface.[5,8,9] This adsorption appears to be a very convenient model reaction for investigating elementary mechanisms of water adsorption at ice surfaces. In this paper we present results of our combined infrared reflection adsorption spectroscopy (IRAS) and quantum chemical studies of water adsorption on the bilayer-terminated ice surface grown on Ru(001).

Experimental Section

The experiments were carried out in an ultrahigh vacuum chamber which was equipped with a three-grid retarding field analyzer for low-energy electron diffraction (LEED) and Auger electron spectroscopy (AES), and a quadrupole mass filter for thermal desorption spectroscopy (TDS). The base pressure was $<1 \times 10^{-10}$ Torr. A Fourier transform infrared spectrometer (Mattson RS-1), a mirror system, and a narrow band mercury cadmium telluride (MCT) detector were coupled to the chamber. A collimated parallel IR beam was focused on the sample at an incident angle of 85° by an off-axis paraboloidal mirror through a BaF_2 window. A Ru(001) clean surface served as a background reference for the absorption spectrum. A resolution of 4 or 8 cm^{-1} and p-polarized light were used for IRAS measurement. Notably, s-polarized light gave no absorption peak for both ice and adsorbate, indicating that the dipole selection rule of IRAS at metal surface works at this surface. All the spectra reported here were recorded at the surface temperature of 38 K. Water gas was introduced by way of a pulsed gas delivery system. The sample was cooled to 38 K using a cryogenic refrigerator and was heated to 150 K by electron bombardment from the rear. The Ru(001) clean surface was prepared by Ar-ion bombardment, annealing, oxidation, and flashing cycles. The cleanliness was confirmed by LEED and AES and also checked using the IRAS spectrum of a CO-covered surface. The heating rate for TDS and IRAS annealing sequences was ∼1 5 K/s. The cooling rate was ∼1 K/s. We prepared the well-crystallized and monohydride-terminated ice surface on Ru(001). The ice film was grown below 100 K. The deposition rate was ∼1/7−1/6 bilayer/s. After the deposition, the film was annealed at ∼125 K. The water coverage was estimated from TDS, assuming that the ice multilayer grows after the saturation of the bilayer growth and that the sticking coefficient of water is independent from the coverage.[1]

Details of Calculations

HF and MP2 calculations were performed with the GAUSSIAN-94 package.[10] The standard 6-31G(d), 6-311G(d,p), and 6-311+G(d,p) basis sets were used. Molecular vibrations were animated with the MOLDEN program.[11]

The ice surface was modeled by a cluster including 12 water molecules (model **1**) of the surface bilayer (Figures 1 and 2).

* Corresponding author.
† University of Stockholm.
‡ The Institute of Physical and Chemical Research.

10.1021/jp012971m CCC: $22.00
Published on Web 02/02/2002

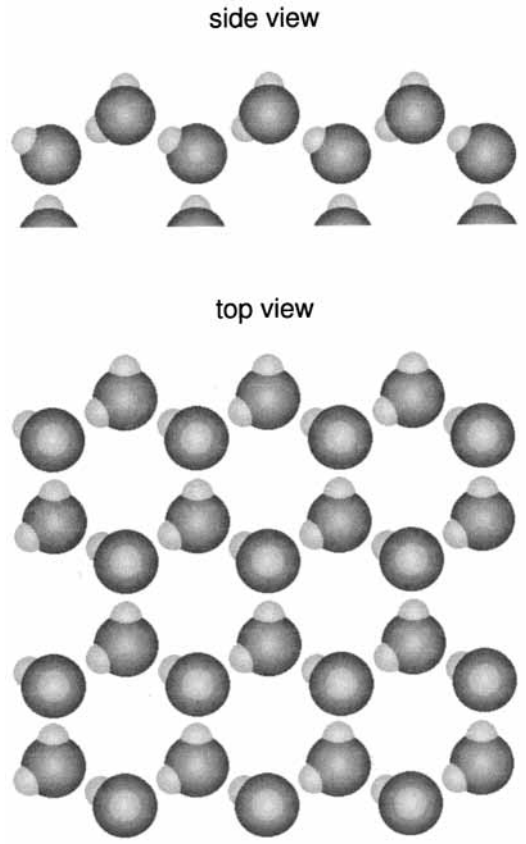

Figure 1. Structure of the bilayer ice surface.

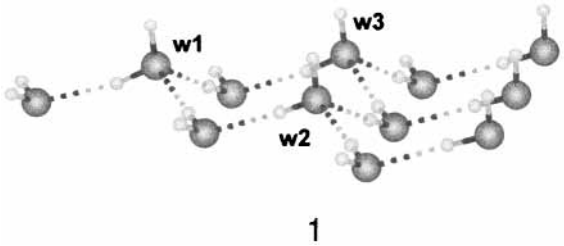

Figure 2. Cluster model of the bilayer ice surface.

The positions of the lower oxygen atoms were fixed, corresponding to the ideal geometry of the 2D lattice with $R_{O-O} = 2.85$ Å. The terminal H atoms of this lower layer were directed toward the nearest O atoms of the neglected lattice. All the remaining geometry parameters were optimized.

Vibrational frequencies were computed within the harmonic approximation. We also assumed that the effect of vibrational coupling between the terminal OH groups of the bilayer surface is insignificant.

Results and Discussion

1. IRAS Data. Figure 3 presents the OH stretching (3800−2900 cm^{-1}) and the HOH bending (1800−1000 cm^{-1}) spectral regions of the ice after annealing (A) and those after the adsorption of 0.14 (B), 0.28 (C), and 0.42 (D) ML of water. Curves B/A, C/A, and D/A show the changes of IRAS bands upon adsorption, being obtained by subtraction of spectrum A from spectra B, C, and D, respectively.

Four OH bands can be distinguished in the stretching region of the spectra: three narrow bands at 3720, 3695, and 3665 cm^{-1} and the very broad, intense band at 3650−3000 cm^{-1}. (Although the intensity of the 3665 cm^{-1} band is comparable to that of the spectral noise, we consider this band to correspond

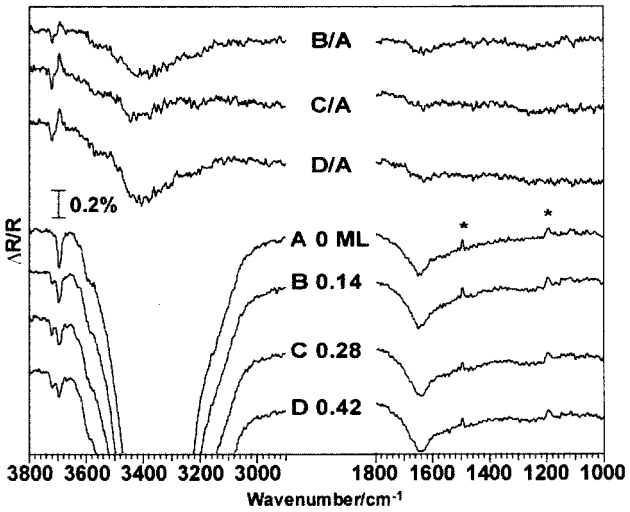

Figure 3. IRAS spectra of clean ice surface (A) and water adsorption on ice for submonolayer coverages (B−D). The difference spectra (B/A, C/A, and D/A) between the clean and the submonolayer water covered spectra are also shown.

to a surface species since it appears in both C and D spectra). Being narrow, the bands at 3720, 3695, and 3665 cm^{-1} should be related to the free OH groups of some adsorbed water species. The 3650−3000 cm^{-1} band is mainly associated with the H-bonded OH groups of the bulk ice (spectra A, B, C, and D).

Only the 3695 cm^{-1} band can be found in the spectrum of the clean surface (spectrum A). According to the ice structure (Figure 1), we assign this band to the stretching vibration of the free surface OH groups (hereafter denoted as HO_s). Upon adsorption the new bands at 3720 and 3665 cm^{-1} appear. The 3720 cm^{-1} band is close in wavenumber to the asymmetric stretching vibration of the proton-acceptor water molecule of the $H_2O\cdots HOH$ dimer[12] (3728 cm^{-1}). Therefore one can tentatively attribute this band to the $H_2O\cdots HO_s$ surface species formed by the adsorption of single water molecules at the free HO_s groups. It is to be noted that the decrease of the 3695 cm^{-1} band of HO_s groups does not linearly correlate with the coverage: no significant change in the intensity of this band occurs in increasing the coverage from 0.28 to 0.42 ML (Figure 3). This fact can be explained by association of the adsorbed molecules into surface clusters and/or by the formation of some adsorbed species which contribute to the same 3695 cm^{-1} band. This implies that the adsorption does not follow the simple mechanism

$$H_2O + HO_s \rightarrow H_2O\cdots HO_s \qquad (1)$$

even when the concentration of HO_s is sufficient enough to accommodate all the adsorbed water molecules as isolated species. Also the appearance of the 3665 cm^{-1} band at 0.28 and 0.42 ML indicates the formation of some water species different from $H_2O\cdots HO_s$. These results contradict the half-bilayer-terminated model of the ice surface[13] corresponding to the stabilization of one isolated water molecule at each of the HO_s groups.

As could be expected, the adsorption increases the intensity of the 3650−3000 cm^{-1} band of the H-bonded water species (cf. the B/A, C/A, and D/A spectra). No individual OH band of adsorbed species can be unambiguously distinguished in this region.

The bending region of the spectra is represented by the broad band at 1650 cm^{-1} only (Figure 3), the sharp bands at 1500 and 1200 cm^{-1} (marked by asterisks) being some contamination

TABLE 1: Frequencies of Water Molecule and Frequency Shifts of Water Dimer (cm^{-1})

molecule	mode	6-31G(d,p)	MP2/6-31G(d,p)	6-311G(d,p)	6-311+G(d,p)	expt[a]
H_2O	ν_{as}	4265	4030	4238	4244	3734
	ν_s	4147	3891	4143	4142	3638
	δ	1769	1682	1750	1726	1589
dimer (1)	$\Delta\nu_{as}$	−25	−32	−24	−22	−26
	$\Delta\nu_s$	−47	−73	−46	−46	−64
	$\Delta\delta$	28	32	29	31	21
dimer (2)	$\Delta\nu_{as}$	−12	−23	−7	−8	−6
	$\Delta\nu_s$	−8	−15	−7	−5	−5
	$\Delta\delta$	0	−2	−1	14	4

[a] Ref 12.

TABLE 2: Frequencies of Methanol and Frequency Shifts of Methanol Dimer (cm^{-1})

molecule	mode	6-31G(d,p)	MP2/6-31G(d,p)	6-311G(d,p)	6-311+G(d,p)	expt
CH_3OH	ν'_{as}	3277	3243	3257	3261	3005[a]
	ν_s	3157	3096	3141	3148	2848[a]
	ν_{OH}	4191	3912	4185	4188	3667[a]
	δ_{OH}	1491	1408	1489	1472	1335[a]
dimer (1)	$\Delta\nu'_{as}$	−19	−20	−19	−19	−13[a]
	$\Delta\nu_s$	−15	−19	−15	−14	−15[a]
	$\Delta\nu_{OH}$	−64	−91	−63	−68	−107[b]
	$\Delta\delta_{OH}$	63	81	63	64	49[c]
dimer (2)	$\Delta\nu'_{as}$	18	15	15	13	
	$\Delta\nu_s$	17	17	17	15	
	$\Delta\nu_{OH}$	5	6	4	1	11[a]
	$\Delta\delta_{OH}$	−4	−10	−4	3	−2[c]

[a] Ref 21. [b] Ref 22. [c] Ref 23.

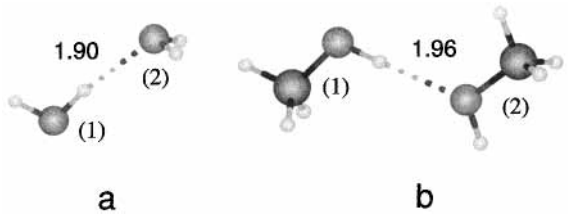

Figure 4. Water (a) and methanol (b) dimers.

bands. No pronounced changes of the 1650 cm^{-1} band can be found after the adsorption. Therefore, similar to the stretching vibrations of the H-bonded OH in the 3650−3300 cm^{-1} region (see above), the bending vibrations of the adsorbed species are useless for the following analysis.

2. Calculation Results. *2.1. Theoretical Approach Used for Frequency Calculations.* Results of theoretical studies by Pulay et al.,[14] Blom et al.,[15] and Botschwina et al.[16] suggest that the HF method with a moderate basis set should correctly describe the *difference in frequency* of a molecular fragment in different chemical environments since the errors in the computed force fields are quantitatively systematic (see also refs 17−19). This feature of the HF approximation has been successfully used for developing the scaled quantum mechanical force field (SQMFF) methodology for the quantitative description of vibrational frequencies of molecules[14−16] and molecular complexes.[20] According to theoretical results by Williams and coauthors,[20] larger basis sets, polarization functions, diffuse functions, or electron correlation should not produce a more accurate prediction of these frequency differences. To illustrate this fact, in Tables 1 and 2 we report the calculated HF stretching frequencies and frequency shifts for H_2O and CH_3OH dimers (Figure 4), respectively. The available experimental values[12,21−23] for these complexes in the gas phase and matrix isolation are also presented. Although for the CH_3 and the OH groups the computed HF/6-31G(d,p) frequencies underestimate the related experimental values by up to ∼500 cm^{-1}, the frequency shifts are reproduced to an average accuracy of 6 cm^{-1} which about corresponds to the accuracy of experimental measurements for these complexes. For the H-bonded OH groups of CH_3OH and H_2O dimers, the HF/6-31G(d,p) method underestimates the experimental shifts by 43 and 17 cm^{-1}, respectively. This is mainly due to the anharmonicity effect which cannot be included within the used harmonic approximation (at the MP2/VTZ-(2df,2p) level[24] the corresponding corrections to $\Delta\nu_{OH}$ for anharmonicity are equal to 35 and 28 cm^{-1}). The calculations of these complexes at the MP2/6-31G(d,p), HF/6-311G(d,p), and HF/6-311+G(d,p) levels suggest that neither inclusion of electron correlation no increase of the basis set should change significantly the results (Tables 1 and 2). Therefore we will calculate the frequencies at the HF/6-31G(d,p) level as

$$\nu^{th} = \nu_o^{exp} + \Delta\nu^{th} \quad (2)$$

for the OH stretching vibrations associated with the free OH groups and the bending vibrations, and as

$$\nu^{th} = \nu_o^{exp} + \Delta\nu^{th} - 28\ cm^{-1} \quad (3)$$

for the OH stretching vibrations corresponding to the H-bonded OH groups, where ν_o^{exp} is the related experimental value for the free molecule and $\Delta\nu^{th}$ is the calculated frequency shift with respect to the free molecule.

2.2. Clean Ice Surface. Table 3 presents the calculated frequencies of the water molecules of the upper layer of model **1** (**w1**, **w2,** and **w3**, Figure 2). The only vibration of these molecules falling in the 3800−3650 cm^{-1} range is the asymmetric stretching mode ν_{as}, which is basically the stretching vibration of the free HO_s groups. The calculated ν_{as} frequencies 3688 (**w1**), 3694 (**w2**), and 3695 (**w3**) cm^{-1} are in very good agreement with the observed band at 3695 cm^{-1} for the clean bilayer-terminated ice surface (Figure 3).

2.3. Adsorption of One Water Molecule. Figure 5 shows the optimized geometry of model **2**, which mimics an isolated water molecule adsorbed on the ice surface. The starting geometry corresponded to the optimized model **1** with molecule **w4** being

TABLE 3: Frequencies of Molecular Models[a] (cm^{-1})

model	mode	w1	w2	w3	w4	w5	w6	expt
1	ν_{as}	3688	3694	3695				3695
	ν_s	3428	3418	3416				
	δ_{OH}	1618	1603	1608				
2	ν_{as}	3570	3695	3696	3723			3695, 3720
	ν_s	3469	3394	3402	3635			
	δ_{OH}	1637	1604	1596	1593			
3(**3′**)	ν_{as}	3554[3559]	3664[3669]	3639[3640]	3695[3694]	3677[3679]		3665, 3695
	ν_s	3455[3431]	3308[3305]	3414[3416]	3502[3488]	3474[3463]		
	δ_{OH}	1605[1608]	1639[1638]	1645[1642]	1631[1635]	1619[1622]		
4	ν_{as}	3563	3613	3679	3698	3680	3691	3695
	ν_s	3437	3409	3370	3503	3453	3558	
	δ_{OH}	1601	1645	1614	1625	1623	1582	

[a] Only the OH stretching frequencies associated with the free OH groups (underlined in the table) can be used for analysis of the structure. All the frequencies corresponding to the OH stretching vibrations of the H-bonded OH groups and the HOH bending vibrations could not be distinguished in the spectra (see the text).

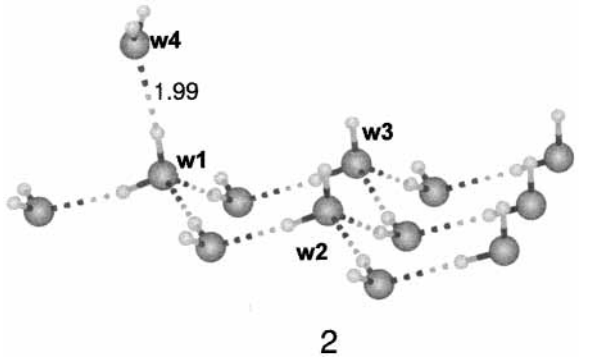

Figure 5. Cluster model of a single water adsorbed on the bilayer ice surface.

H-bonded with the HO_s group of molecule **w1** of the upper layer ($R_{O(w4)-H(w1)}$ = 1.8 Å, ∠O(**w4**)H(**w1**)O(**w1**) = 180°). This adsorption forms two new water species compared to the clean surface (model **1**): the H-bonded water molecule of the upper layer (**w1** molecule of model **2**) and the adsorbed water molecule itself (**w4** molecule of model **2**). The calculated binding energy for this adsorption is equal to 8.7 kcal/mol. The computed frequencies of species **w1**, **w2**, **w3**, and **w4** of model **2** are listed in Table 3. According to these frequencies, the only new OH stretching band which should emerge in the 3800−3650 cm^{-1} region as a result of this type of adsorption is the ν_{as} band of species **w4** at 3723 cm^{-1}. This theoretical prediction is in excellent agreement with the appearance of the 3720 cm^{-1} band after the adsorption of the first dose of water (spectrum B, Figure 3). Therefore we conclude that the ν_{as} mode of the isolated species **w4** contributes to the 3720 cm^{-1} band in the IRAS spectra. Since the formation of species **w4** involves the HO_s sites, the intensity of the 3695 cm^{-1} band of these sites decreases in going from 0 to 1/7 ML (Figure 3).

2.4. Adsorption of Two Water Molecules on Neighboring Surface OH Groups. Figure 6 shows the optimized geometry of model **3** corresponding to the adsorption of two water molecules on the neighboring HO_s sites (molecules **w4** and **w5** of model **3**). The starting geometry was analogous to that of model **2** with the additional water molecule **w5** being H-bonded to the HO_s group of the surface molecule **w2** ($R_{O(w5)-H(w2)}$ = 1.8 Å, ∠O(**w5**)H(**w2**)O(**w2**) = 180°). In the optimized structure molecules **w4** and **w5** are H-bonded with each other. During the optimization molecule **w5** loses its initial, strong H-bond with the surface but forms three new H-bonds, namely the strong H-bond with the adsorbed molecule **w4** and two weak H-bonds with the surface molecules **w2** and **w3**. The calculated total

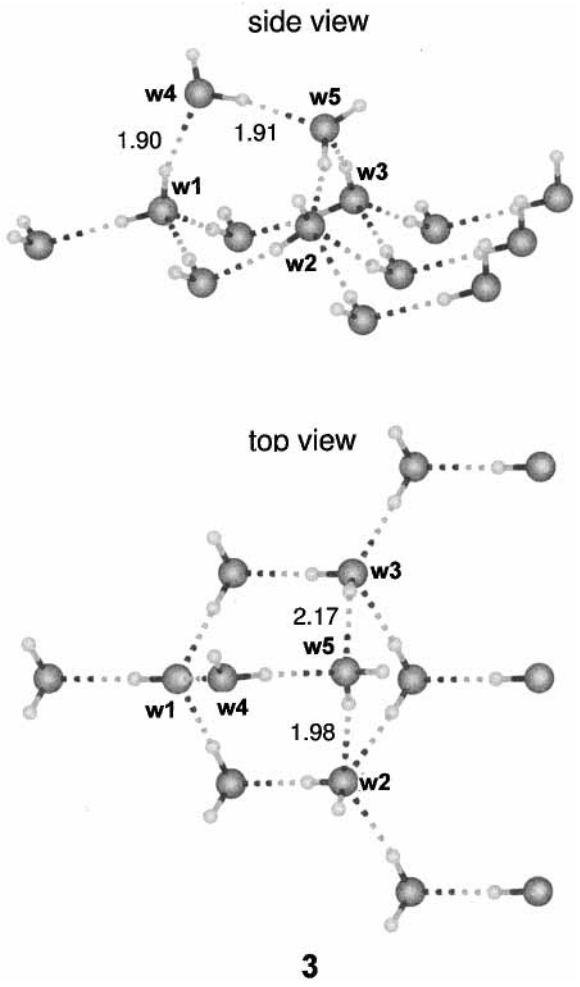

Figure 6. Cluster model of the adsorption of two water molecules on the neighboring OH groups of the bilayer ice surface.

binding energy for this adsorption is 23.8 kcal/mol (11.9 kcal/mol per water molecule). Since for two isolated water species (molecule **w4**, model **2**) the total binding energy is equal to 17.4 kcal/mol, the H-bonding interaction between the two water molecules adsorbed at the neighboring HO_s groups increases the total stabilization energy by 6.4 kcal/mol. This result implies that the half-bilayer terminated surface structure[13] is strongly energetically unfavorable.

Although the interaction between molecules **w4** and **w5** significantly deviates the O(**w1**)−H(**w1**)···O(**w4**) angle from its optimal value of about 180° for the H(**w1**)···O(**w4**) H-bond

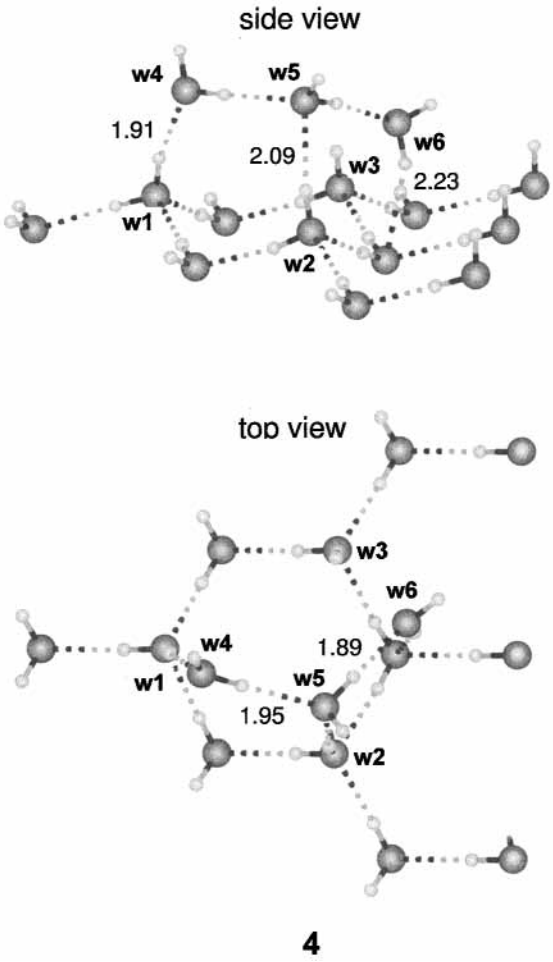

Figure 7. Cluster model of the adsorption of three water molecules on the neighboring OH groups of the bilayer ice surface.

(cf. models **2** and **3**), this H-bond strengthens (cf. the bond lengths). This is due to the cooperative effect between the H-bonds in the [···OH(**w1**)···OH(**w4**)···OH(**w5**)··] surface polymer.

The computed frequencies of species **w1**, **w2**, **w3**, **w4**, and **w5** of model **3** are reported in Table 3. Only three of the computed OH stretching frequencies of these species turn out to be in the 3800−3650 cm^{-1} spectral region, namely the 3695 (**w4**), 3677 (**w5**), and 3664 (**w2**) cm^{-1} frequencies. The 3695 cm^{-1} frequency of molecule **w4** exactly corresponds to the position of the ν_{as} stretching band of the free HO_s groups. This result conforms to the experimental fact that the decrease in the intensity of the 3695 cm^{-1} band of the HO_s groups does not linearly correlate with the coverage suggesting that this is due to the formation of a water species which contributes to the same 3695 cm^{-1} band. The difference between the 3677 (**w5**) and 3695 (HO_s) cm^{-1} frequencies is comparable to the width of the 3695 cm^{-1} band (∼20 cm^{-1}) and the concentration of species **w5** is small compared to the concentration of HO_s groups. Therefore the 3677 cm^{-1} mode of molecules **w5** should not manifest itself as a separate OH band but be a small component of the 3695 cm^{-1} band. The 3664 cm^{-1} frequency of species **w2** nearly coincides with the 3665 cm^{-1} band in the spectra. Therefore we assign this band to the free HO_s surface groups acting as a proton acceptor toward the adsorbed water species.

2.5. Adsorption of Three Water Molecules on Neighboring Surface OH Groups. Figure 7 shows the optimized geometry of model **4** mimicking the adsorption of three water molecules on the neighboring HO_s groups. The initial geometry of this model was similar to that of model **3** with the additional molecule **w6** being H-bonded with the surface molecule **w3** ($R_{O(w6)-H(w3)}$ = 1.8 Å, ∠O(**w6**)H(**w3**)O(**w3**) = 180°). In the final structure the adsorbed molecules form the [···OH(**w1**)··· OH(**w4**)···OH(**w5**)···OH(**w6**)··] chain of H-bonded OH group providing the maximum cooperative effect between these molecules. The computed total binding energy for this adsorption is equal to 36.6 kcal/mol (12.1 kcal/mol per water molecule). Both models **3** and **4** suggest a strong tendency of the adsorbed water molecules to form water clusters on the bilayer-terminated ice surface. The relative arrangement of water molecules in these clusters is dominated by both the inter-cluster and the surface-cluster interactions being significantly different from that in the bulk ice.

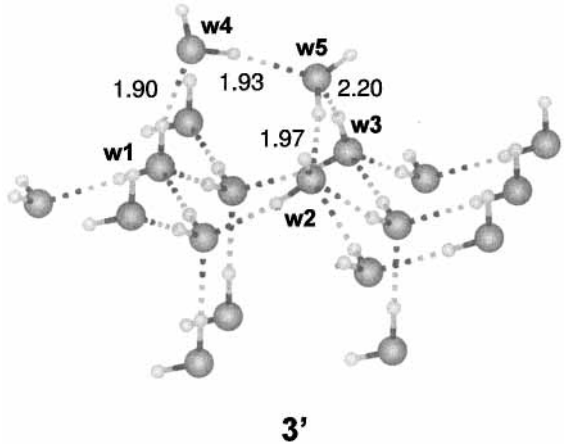

Figure 8. Extended cluster model of the adsorption of two water molecules on the neighboring OH groups of the bilayer ice surface.

The calculated frequencies of molecules **w1**, **w2**, **w3**, **w4**, **w5**, and **w6** of model **4** are listed in Table 3. Four asymmetric stretching vibrations of these molecules lay in the 3800−3650 cm^{-1} region. These are the 3698 (**w4**), 3691 (**w6**), 3680 (**w5**), and 3679 (**w3**) cm^{-1} vibrations. The difference in frequency between these vibrations and the asymmetric stretching vibration of the HO_s surface groups is within 16 cm^{-1} only. Therefore these modes should not appear as separate OH bands in the spectra but contribute to the 3695 cm^{-1} band of HO_s groups.

2.6. Effect of Model Size. To check whether the calculated binding energies and frequencies can significantly depend on the size of the model, the adsorption of two water molecules on the neighboring HO_s sites was calculated also with model **3′** (Figure 8), which is an extended analogue of model **3**. The positions of five additional water molecules of model **3′** (compared to model **3**) correspond to the idealized ice structure. The total stabilization energy 25.2 kcal/mol (12.6 kcal/mol per one molecule) for model **3′** is close to that of 23.8 kcal/mol (11.9 kcal/mol per one molecule) for model **3**. Also the difference in geometry and frequencies between models **3** and **3′** are insignificant (cf. Figures 6 and 8, and Table 3). These results suggest that a further extension of the model size should not affect the results.

Conclusion

Our combined infrared and quantum chemical study indicates a significant role of the lateral H-bonding interaction between the neighboring water molecules adsorbed on the bilayer terminated ice surface. As an example, for two adjacent water molecules the energy gain due to this interaction is about 6 kcal/

mol. This interaction leads the neighboring adsorbed water molecules to aggregate with the structure of the formed surface clusters being significantly different from that of the ice. This implies that upon adsorption of water the growth of the ice should occur by successive phase transitions from the disordered adsorption layer to the ordered ice lattice.

Our calculations suggest four different water species associated with three bands in the infrared spectra. These are the single water molecules adsorbed at the terminal surface OH groups (asymmetric stretching mode at 3720 cm^{-1}), the water molecules of the upper layer of the ice surface (stretching mode of the free OH group at 3695 cm^{-1}), the water molecules of the clusters having a free OH group (stretching mode of the free OH groups at 3695 $\pm$ 20 cm^{-1}), and the water molecules of the upper surface layer of ice interacting with adsorbed species by the oxygen atom (stretching mode of the free OH group at 3665 cm^{-1}).

Acknowledgment. A.P. thanks the Swedish Foundation for International Cooperation in Research and Higher Education (STINT) for funding. Grants of computer time from the PDC and NSC supercomputer centers are gratefully acknowledged.

References and Notes

(1) Thiel, P. A.; Madey, T. E. *Surf. Sci. Rep.* **1987**, *7*, 211.

(2) Morgenstern, M.; Michely, T.; Comsa, G. *Phys. Rev. Lett.* **1996**, *77*, 703.

(3) Glebov, A.; Graham, A. P.; Menzel, A.; Toennies, J. P. *J. Phys. Chem.* **1997**, *106*, 9382.

(4) Schmitz, P. J.; Polta, J. A.; Chang, S. L.; Thiel, P. A. *Surf. Sci.* **1987**, *186*, 219.

(5) Ogasawara, H.; Yoshinobu, J.; Kawai, M. *Chem. Phys. Lett.* **1994**, *231*, 188.

(6) Ogasawara, H.; Yoshinobu, J.; Kawai, M. *J. Chem. Phys.* **1999**, *111*, 7003.

(7) Anderson, A. B. *Surf. Sci.* **1981**, *105*, 159.

(8) Jo, S. K.; Polanco, J. A.; White, J. M. *Surf. Sci.* **1991**, *253*, 233.

(9) Fisher, G. B.; Gland, J. C. *Surf. Sci.* **1980**, *94*, 446.

(10) Frisch, M. J.; Trucks, G. W.; Schlegel, H. B.; Gill, P. M. W.; Johnson, B. G.; Robb, M. A.; Cheeseman, J. R.; Keith, G. A.; Petersson, D. A.; Montgomery, J. A.; Al-Laham, M. A.; Zakrzewski, V. G.; Ortiz, J. V.; Foresman, J. B.; Cioslowski, J.; Stefanov, B. B.; Nanayakkara, A.; Challacombe, M.; Peng, C. Y.; Ayala, P. Y.; Chen, W.; Wong, M. W.; Andres, J. L.; Replogle, E. S.; Gomperts, R.; Martin, R. L.; Fox, D. J.; Binkley, J. S.; Defrees, G. J.; Baker, J.; Stewart, J. P.; Head-Gordon, M.; Gonzalez, C.; Pople, J. A. GAUSSIAN 94 (Revision A.1); Gaussian, Inc.: Pittsburgh, PA, 1995.

(11) Schaftenaar, G. MOLDEN, CAOS/CAMM Center, The Netherlands.

(12) Engdahl, A.; Nelander, B. *J. Mol. Struct.* **1989**, *193*, 101.

(13) Materer, N.; Starke, U.; Barbieri, A.; van Hove, M. A.; Somorjai, G. A.; Kroes, G.-J.; Minot, C. *Surf. Sci.* **1997**, *381*, 190.

(14) Pulay, P.; Fogarasi, G.; Pongor, G.; Boggs, J. E.; Vargha, A. *J. Am. Chem. Soc.* **1983**, *105*, 7037.

(15) Blom, C. E.; Altona, C. *Mol. Phys.* **1976**, *31*, 1377.

(16) Botschwina, P. *Chem. Phys. Lett.* **1974**, *29*, 98.

(17) Pelmenschikov, A.; Morosi, G.; Gamba, A.; Coluccia, S. *J. Phys. Chem.* **1995**, *99*, 15018.

(18) Pelmenschikov, A.; Morosi, G.; Gamba, A.; Coluccia, S. *J. Phys. Chem. B* **1998**, *102*, 2226.

(19) Pelmenschikov, A.; Morosi, G.; Gamba, A.; Coluccia, S.; Martra, G.; Pettersson, L. G. M. *J. Phys. Chem. B* **2000**, *104*, 11497.

(20) Williams, R. W.; Chen, J. L.; Weir, A. F. *J. Phys. Chem.* **1995**, *99*, 5299.

(21) Barnes, A. J.; Hallam, H. E. *Trans. Faraday Soc.* **1970**, *66*, 1920.

(22) Huisken, F.; Kulcke, A.; Laush, C.; Lisy, J. M. *J. Chem. Phys.* **1991**, *95*, 3924.

(23) Murto, J.; Räsänen, M.; Aspiala, A.; Kemppinen, E. *Acta Chem. Scand.* **1983**, *A37*, 323.

(24) Bleiber, A.; Sauer, J. *Chem. Phys. Lett.* **1995**, *238*, 243.